Onset of wavy vortices in Taylor-Couette flow with imperfect reflection symmetry

J. Abshagen and G. Pfister
Institute of Experimental and Applied Physics, University of Kiel, 24098 Kiel, Germany
(Received 3 July 2007; revised manuscript received 16 August 2008; published 16 October 2008)

We reveal experimentally a mechanism that alters the critical behavior of a Hopf bifurcation substantially due to the presence of imperfections of the reflection symmetry in a hydrodynamic system. The onset of rotating waves in Taylor vortex flow, which is widely considered as a "classical" example for a Hopf bifurcation in hydrodynamics, is investigated primarily by transient response experiments. While wavy vortex flow is not influenced by such (unavoidable) experimental imperfections, the critical behavior of the axially subharmonic rotating wave with wavy outflow boundaries, also called the small-jet mode, is qualitatively altered. Experimental evidence is provided that the modified critical behavior at the Hopf bifurcation is associated with imperfections of the reflection symmetry of the Taylor-Couette setup. The experimental results on Hopf bifurcation are discussed in the context of a cusp-Hopf bifurcation model recently proposed by Harlim and Langford [Int. J. Bifurcation Chaos Appl. Sci. Eng. **17**, 2547 (2007)] and compared to experimental results on imperfect pitchfork bifurcation in small-aspect ratio Taylor-Couette flow.

DOI: 10.1103/PhysRevE.78.046206 PACS number(s): 05.45.−a, 47.20.Ky, 02.30.Oz

I. INTRODUCTION

Bifurcations play an important role in the organization of complex dynamics and pattern formation in many nonlinear systems [1,2]. An in-depth knowledge of the relevant symmetries is of crucial importance for the understanding of a bifurcation event [3]. Since experimental systems are never perfectly symmetric, as assumed generally in models of the physical system, a realistic description of a bifurcation event in a physical system has to cope with the influence of imperfections which break these symmetries. Imperfection theory has successfully been applied in order to model bifurcation events in physical systems, e.g., with imperfect reflection symmetry, such as pitchfork [4] or gluing bifurcations [5,6].

Modern ideas from bifurcation theory have been very succesful in the interpretation of behavior close to hydrodynamic instabilities in many fluid flows [2,7], such as in the Taylor-Couette system [8]. Taylor-Couette flow is the flow of a viscous liquid in the gap between two concentric, rotating cylinders. The "classical" experimental system with rotating inner and nonrotating outer cylinder as well as nonrotating rigid end plates is invariant under azimuthal rotations and has an axial reflection symmetry. The onset of rotating waves in axisymmetric Taylor vortex flow, the so-called "wavy vortex flow" or more generally "wavy Taylor vortex flow," serves as one of the classical example for a Hopf bifurcation in hydrodynamics (see, e.g., [2,3,7,8]). Rotating waves break the azimuthal rotational invariance, but keep a (spatial or spatiotemporal) reflection symmetry in the absence of experimental imperfections.

Hopf bifurcations often provide an appropriate description for the onset of time dependence and the appearance of oscillatory patterns in systems with symmetries (see, e.g., [2,3]). Though imperfections can alter the structure of a Hopf bifurcation with symmetry [9,10] in principle, a simple reflection symmetry like in the Taylor-Couette system and the corresponding imperfections generally do not influence the behavior of a Hopf bifurcation [3].

In this work experimental results are presented which show that the behavior near a Hopf bifurcation can substantially be influenced by the presence of imperfections of the reflection symmetry.

The experimental results suggest a coupling of the Hopf bifurcation towards wavy Taylor vortices to reflection symmetry breaking. Although no bifurcation point of higher codimension is observed, the presence of (damped) symmetry breaking is found to have a crucial influence on the Hopf bifurcation. A recently proposed cusp-Hopf bifurcation model by Harlim and Langford [11] suggest that such a coupling of a Hopf bifurcation to symmetry breaking is a consequence of imperfection of the reflection symmetry and would be absent in a perfectly symmetric system. Examples for Hopf bifurcations coupled to additional slow modes arise in various systems, such as in chemical systems [12], from advected fields [13], from conservation laws [14], and from Goldstone modes due to broken translational invariance [15].

II. WAVY TAYLOR VORTICES

Axisymmetric Taylor vortices have the form of axial pairs of counterrotating, toroidal vortices and thus leave the flow invariant under azimuthal rotation and, also, in a classical Taylor-Couette system, symmetric with respect to axial reflections [8]. They appear smoothly in the laminar flow of the Taylor-Couette system for Reynolds numbers close to the centrifugal instability of the mathematical system, and their number as well as the exchange process depends strongly on the aspect ratio [16]. The aspect ratio—i.e., the axial length normalized by the gap width—as well as the radius ratio and the Reynolds number serve as control parameters of Taylor-Couette flow.

At higher Reynolds numbers axisymmetric Taylor vortices can become unstable via a Hopf bifurcation towards time-dependent flows which have the form of a rotating wave [17–20]. The rotating waves have an azimuthal wave number $m>0$ and wave speed c, and they break the rotational invariance of the system; i.e., the flow becomes nonaxisymmetric. Rotating waves appear as a steady flow in a certain corotating frame. The classical wavy vortex flow—

i.e., the collective axial motion at any azimuthal position with azimuthal periodicity—is predominant in small-gap Taylor-Couette flow, but depending on the aspect ratio and the radius ratio, rotating waves of different wave speed, azimuthal wave number, and axial periodicity can occur [17]. The predominant rotating waves in Taylor-Couette flow with a radius ratio of 0.5 are, additionally to the wavy mode, the so-called small-jet mode [18]. This mode has also been labled as "wavy outflow boundary" [19] and "subharmonic mode" [20] since the oscillation amplitude is localized in the outward jets and adjacent outward jets oscillate in antiphase; i.e., the flow is axially subharmonic with respect to the period of Taylor vortices. The wavy mode and the small-jet mode both have a reflection symmetry which is either spatiotemporal or purely spatial as for the small-jet mode in the case of an even number of Taylor vortex pairs. The small-jet flow state can break the reflection symmetry well beyond the critical point in a symmetry-breaking pitchfork bifurcation [21]. Such bifurcation behavior is not observed for the wavy mode.

III. EXPERIMENTAL SETUP

The measurements are performed in a Taylor-Couette setup with a rotating inner and a nonrotating outer cylinder. The rotating inner cylinder is machined from stainless steel having a radius of $r_i=(12.50\pm0.01)$ mm, while the stationary outer cylinder is made from optically polished glass with a radius of $r_o=(25.00\pm0.01)$ mm. At top and bottom the fluid is confined by metal end plates, which are held fixed in the laboratory frame. The distance between these plates defines the axial height L of the flow, which is adjustable within an accuracy of 0.01 mm up to a maximal height of 250.00 mm. Geometric parameters of Taylor-Couette flow are the aspect ratio $\Gamma=L/d$, with gap width $d=r_o-r_i$, and the radius ratio $\eta=r_i/r_o$ which is held fixed to $\eta=0.5$ for all measurements. The control parameter serves as the Reynolds number, which is $\mathrm{Re}=2\pi f d r_i/\nu$, with f denoting the rotation frequency of the inner cylinder. With a (PLL) phase-locked loop control an accuracy of $\Delta f/f\propto10^{-4}$ in the short-term and $\Delta f/f\propto10^{-7}$ in the long-term average is achieved. As a working fluid within the gap between the two concentric cylinders, a silicone oil with a kinematic viscosity ($\nu=11.9\pm0.1$) cSt is used. The uncertainty of ±0.1 cSt refers to the measurement of the absolute value of kinematic viscosity. The accuracy of ν during a measurement is primarily determinated by the temperature variation of the fluid that is thermostatically controlled to $(21.00\pm0.01)^\circ$ C. This yields a $\Delta\nu=\frac{\partial\nu}{\partial T}\big|_{21.00^\circ\mathrm{C}}\,\Delta T\approx0.0025$ cSt. Although the uncertainty in the absolute value of ν introduces an uncertainty of $\Delta\mathrm{Re}_{abs}/\mathrm{Re}\propto10^{-2}$ in the absolute value of Re, the variation in Reynolds number with time is within $\Delta\mathrm{Re}/\mathrm{Re}\propto10^{-4}$ during a measurement. This variation determinates the resolution in Re that is achieved in the experiment. We utilize laser-Doppler velocimetry (LDV) for contact-free measurements of the axial component v_z of the local flow velocity.

IV. BIFURCATIONS WITH IMPERFECT REFLECTION SYMMETRY

A. Critical slowing down

An investigation of transient dynamics close to a bifurcation provides important information about the properties of a bifurcation event. In particular, it may give insight into the departure from a bifurcation model (see [22,23] for transient dynamics at the onset of Taylor vortices).

The critical slowing down—i.e., the divergence of time constants as the control parameter approaches the critical point—is a typical dynamical phenomenon that occurs close to local bifurcations, such as pitchfork and Hopf bifurcations. Critical slowing down at Hopf bifurcations in fluid-flow experiments has been observed, e.g., at the onset of wavy vortex flow by Pfister and Gerdts [24] and at the onset of oscillations in magnetoconvection by Hof and Mullin [25].

The transient dynamics of a Hopf bifurcation is determined by the slow temporal variations of the oscillation amplitude $A\geqslant0$, which is governed by the Landau amplitude equation

$$\tau_0\frac{dA}{dt}=\varepsilon A-\frac{A^3}{A_0^2}. \tag{1}$$

The same equation governs the critical dynamics at a pitchfork bifurcation in systems with reflection symmetry (in this case A represents symmetry breaking and can therefore also be negative). The relative distance from the critical Reynolds number Re_c is represented by $\varepsilon=(\mathrm{Re}-\mathrm{Re}_c)/\mathrm{Re}_c$, while τ_0 and A_0 are scaling factors for time and amplitude, respectively. A Landau time constant can be defined as $\tau_l:=\tau_0/\varepsilon$, a final amplitude as $A_f:=A_0\sqrt{\varepsilon}$ (for $\varepsilon\geqslant0$), and an initial amplitude as $A_i=A(t=0)$. For supercritical $\varepsilon\geqslant0$ as considered in the following experiments the solution of Eq. (1) is given by

$$A(t)=\frac{A_f e^{t/\tau_l}}{\sqrt{e^{2t/\tau_l}+(A_f/A_i)^2-1}}. \tag{2}$$

An amplitude governed by Landau theory has properties which can be tested experimentally: (i) the square-root-law, i.e., the final amplitude scales with $A_f\propto\sqrt{\varepsilon}$; (ii) the critical slowing down, i.e., the time constant scales with $\tau_l\propto1/\varepsilon$; and (iii) the time constant τ_l depends only on ε and is independent of the initial amplitude A_i.

The latter point has not been paid much attention to in experiments until recently when a significant difference between time constants for onset and decay of Taylor vortices was revealed [23]. It has become apparent from those investigations that the dependence of the time constant from initial conditions may be important to characterize a departure from a bifurcation model. Note that generally the time evolution described by Eq. (2) can significantly differ with A_i, although τ_l may be the same.

In order to obtain an estimate τ for the Landau time constant τ_l from an amplitude relaxation processes, the solution (2) of Landau equation (1) is fitted to experimental time series. The response experiments are performed by a sudden, but small change in Reynolds number close to the onset of nonaxisymmetric waves in steady Taylor vortex flow. As initial conditions serve steady and time-dependent flow states which have been relaxated to their final state at the respective initial Reynolds number Re_i. After a sudden change of the Reynolds number to Re_f, the axial velocity in axial middle of

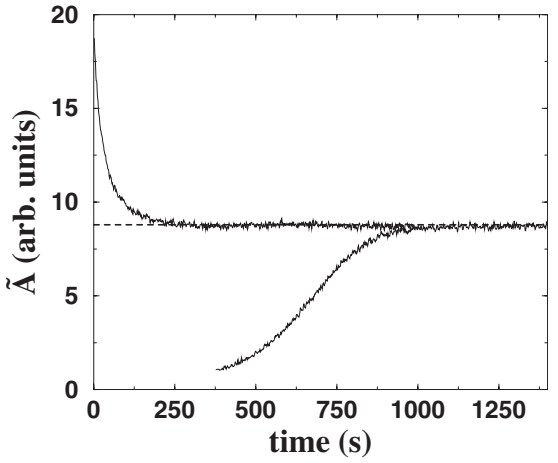

FIG. 1. (a) Transient dynamics of measured amplitude $\tilde{A}$ at the onset (Re_i=344.8) and decay (Re_i=410.6) of wavy vortex flow towards the supercritical final amplitude $\tilde{A}_f$ (dashed line) at Re_f =384.7 in a flow with 16 Taylor cells at Γ/N=1.3.

the cylinder at a distance of 3 mm from the inner cylinder is recorded as a measure of the transient response of the flow. The time series are recorded until the flow has relaxated to the final state at the final Reynolds number Re_f. A LDV measurement volume in the axial middle of the cylinder ensures a linear and symmetric measure of the oscillations due to a linear profile of the axial velocity [21].

Since the slow relaxation of the wave amplitude represents the interesting dynamical quantity close to a Hopf bifurcation, the fast oscillations are not considered in the following. The estimate $\tilde{A}$ of the amplitude A is determined from the extrema of the oscillations. Two new time series are generated from both the maxima $\tilde{A}_{max}(t_i)=\max(A(t))$ and the minima $\tilde{A}_{min}(t_j)=|\min(A(t))|$. The mean of the two (interpolated) time series $\tilde{A}_{min/max}(t)$ yields the estimated amplitude $\tilde{A}(t)$. Typical time series of the estimated amplitude $\tilde{A}$ obtained from transient response experiments at the onset ($\mathrm{Re}_i<\mathrm{Re}_c<\mathrm{Re}_f$) and the decay ($\mathrm{Re}_c<\mathrm{Re}_f<\mathrm{Re}_i$) of wavy vortices are shown in Fig. 1.

B. Dynamics at imperfect pitchfork bifurcation

The behavior of a pitchfork bifurcation can also be described by a Landau amplitude equation (1) in case of a perfect reflection symmetry. While imperfections in the reflection symmetry generally do not influence the behavior close to a Hopf bifurcation, such imperfections have a significant influence on the structure of a pitchfork bifurcation. One of the stable branches is decoupled in a fold bifurcation, while the other stable branch changes smoothly from sub-to supercritical values without passing a critical point on the solution curve. This behavior is described appropriately by an additional term reflecting the symmetry-breaking imperfections in the Landau amplitude equation (see, e.g., [1]):

$$\tau_0 \frac{dA}{dt} = \varepsilon A - \frac{A^3}{A_0^2} + \delta. \tag{3}$$

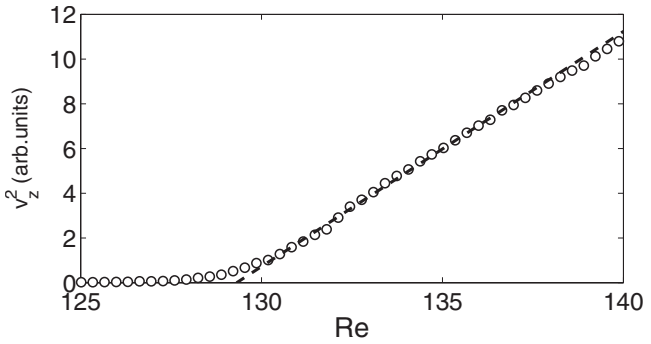

FIG. 2. Continuous branch of an imperfect symmetry-breaking pitchfork bifurcation from symmetric two-cell to asymmetric one-cell flow measured in an experimental system with Γ=1 by the square of the axial velocity, v_z^2, in the axial midplane $z=L/2$ at a radial position $r=r_i$+1.55 mm. The linear fit corresponds to square-root behavior.

In Fig. 2 the smooth onset of an asymmetric steady one-cell flow from a symmetric steady two-cell flow in an experimental system with Γ=1 is shown. In a perfectly symmetric system, as represented by a numerical model of the Navier-Stokes equation with appropriate boundary conditions, this onset is governed by a symmetry-breaking pitchfork bifurcation, but in experimental systems this bifurcation is decoupled due to (unavoidable) imperfections [26]. Although a square-root behavior provides approximately a reasonable description over a wide range of Reynolds numbers, as indicated by the linear fit in Fig. 2, a departure from this scaling law can be seen in particular very close to onset due to imperfections.

Since this departure appears to be small, it might considered as appropriate to apply the fitting procedure described in Sec. IV A in order to extract time constants. In Fig. 3(a) the results of transient response measurements close to symmetry breaking are shown. It can be seen that the time constants significantly depart from the $\tau \propto 1/\varepsilon$ scaling behavior, which would be expected for critical slowing down. The departure increases closer to the critical point, and the onset (●) is significantly more affected than the decay (○). This behavior can be reproduced in numerical simulations of the Landau amplitude equation with imperfection term—i.e., Eq. (3)—as shown in Fig. 3(b).

The significant departure from critical slowing down in experiment (and model) reflects the change in structure of the pitchfork bifurcation due to imperfections. While in the case of perfect reflection symmetric the flow becomes critical as the Reynolds number is changed from sub-to supercritical values, a critical point does not exist on the continuous branch in an imperfectly symmetric system; i.e., no critical slowing down occurs.

C. Hopf bifurcation and imperfect reflection symmetry

Hopf bifurcations in systems with a simple reflection symmetry, such as in Taylor-Couette flow with nonrotating end plates, are structurally stable [3], and therefore imperfections do generally not alter the critical dynamics close to Hopf bifurcation. This is in contrast to the behavior of a

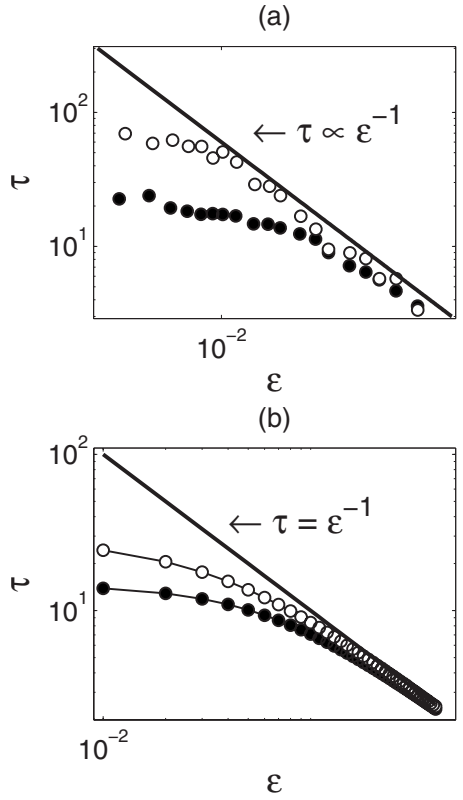

FIG. 3. Time constants τ (onset, ●; decay, ○) determined by fitting procedure (Sec. IV A) from (a) measurements on symmetry-breaking pitchfork bifurcation from symmetric two-cell to asymmetric one cell flow at $\Gamma=1$ and (b) from numerical simulations of Landau amplitude equation [Eq. (3) with $\tau_0=A_0=1$] with a small imperfection term $\delta=0.005$.

symmetry-breaking pitchfork bifurcation that is structurally unstable [3] and therefore the critical divergence of time constants—i.e., critical slowing down—disappears in the presence of imperfections.

However, in the presence of higher symmetries, such as O(2) symmetry [10], or of mode coupling, imperfections in the reflection symmetry can have an influence on a Hopf bifurcation. Harlim and Langford [11] recently investigated the cusp-Hopf bifurcation. The truncated normal form reads [11]

$$\dot{r} = \varepsilon r + r(a_2 r^2 + a_3 z^2) + a_1 z r, \tag{4}$$

$$\dot{z} = \alpha z + z(b_3 z^2 + b_4 r^2) + b_1 r^2 + \beta, \tag{5}$$

where r represents the amplitude of the oscillatory mode, while z the symmetry breaking. For $a_1=b_1=\beta=0$ the system reduces to a pitchfork-Hopf bifurcation which is appropriate to describe mode coupling in systems with perfect reflection symmetry [27]. For $r=0$—i.e., no oscillations are present—the z equation reduces to a simple imperfect pitchfork bifurcation. The term β reflects the effect of symmetry-breaking imperfections which are independent of the oscillation amplitude. The coefficients a_1 and b_1 correspond to quadratic terms which describe couplings in a system where the reflection symmetry is broken. While b_1 also reflects symmetry-breaking imperfections on the pitchfork bifurcation which depend on the oscillation amplitude, the coefficient a_1 reflects variations in the control parameter ε depending on symmetry breaking. Therefore, in a system governed by a cusp-Hopf normal form the presence of symmetry-breaking imperfections can in principle influence the behavior of a Hopf bifurcation due to nonlinear coupling even if symmetry breaking is linearly damped; i.e., $\alpha<0$. This coupling is absent in a perfectly symmetric system.

In order to illustrate this behavior of nonlinear asymmetric coupling in the case of linearly damped symmetry breaking, numerical simulations of Eqs. (4) and (5) are performed. It is focused only on the nonlinear asymmetric coupling a_1 (=0.5) and b_1 (=1.0) while the constant term in the z equation $\beta=0$ is set to zero. For simplicity, the nonlinear damping in the z equation is also set to zero ($b_3=b_4=0$), since z is assumed to be linearly damped ($\alpha=-0.5$), as well as nonlinear damping in the r equation; i.e., $a_3=0$. Furthermore, the nonlinear damping in the r equation is set to $a_2=1$. Scaling behavior is investigated in the interval $\varepsilon \in [0.05:0.4]$ in steps of $\Delta\varepsilon=0.025$. This choice of parameters results in a simple scaling behavior of the final solutions r_f and z_f; i.e., the amplitude of the oscillation still obeys a square-root law $r_f \propto \sqrt{\varepsilon}$, while the symmetry breaking scales linearly $z_f \propto \varepsilon$.

An example of transient dynamics in given in Fig. 4(a). While the onset and decay of the oscillation amplitude $r(t)$ are similar to Landau dynamics in principle, as shown, e.g., in Fig. 1, a significant difference can be seen from Fig. 4(a). An overshooting occurs in the time series for the onset and decay, which is in contrast to purely relaxating dynamics governed by the Landau amplitude equation. The symmetry breaking follows the dynamics of the oscillation amplitude due to the nonlinear coupling.

Although a qualitative difference to the purely relaxating Landau dynamics can be found in the coupled system, the scaling behavior of the onset is only slightly affected. In Fig. 4(b) time constants are shown which are obtained from transients, as shown, e.g., in Fig. 4(a), by applying the fitting procedure in described in Sec. IV A. The scaling behavior for the onset (●) is similar to the critical behavior of the symmetric system—i.e., to $\tau=1/\varepsilon$. While the decay (○) also reveals a critical slowing down, the time scale τ_0 is underestimated by the fitting procedure; i.e., the straight line is located significantly below the theoretical one in Fig. 4(b).

V. ONSET OF ROTATING WAVES

A. Wavy vortex flow

Pfister and Gerdts [24] have studied the transient response at the onset of wavy vortex flow in a Taylor-Couette flow with $\eta=0.5$. They have found experimental evidence for the square-root law of the final amplitude $A_f \propto \sqrt{\varepsilon}$ as well as a critical slowing down with a scaling of the time constants $\tau_l \propto 1/\varepsilon$.

We have extended their study on wavy vortex flow by an investigation of the dependence of the time constants from the initial amplitude. The measurements were performed in a Taylor-Couette flow with 16 cells at a normalized aspect ratio $\Gamma/N=1.3$. The scaling of the final amplitude $\tilde{A}_f^2$ with Re

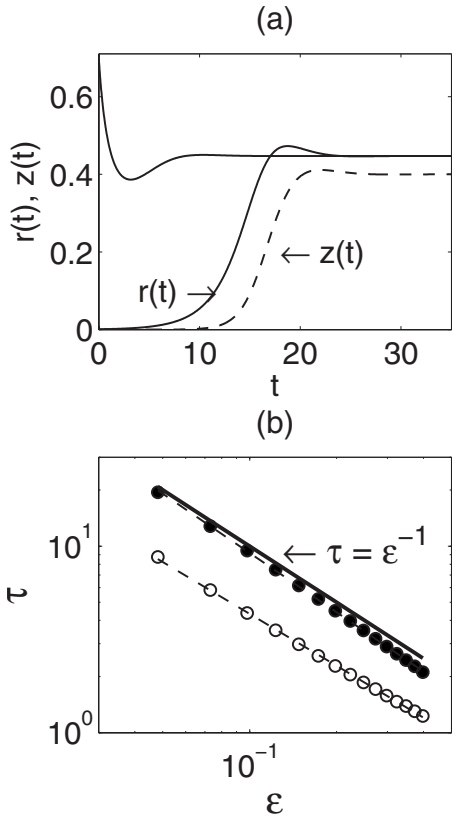

FIG. 4. (a) Examples for transients $r(t)$ (solid line) and $z(t)$ (dashed line) at onset and decay [here only $r(t)$ is shown]. The time series are obtained from numerical simulations of the truncated normal form [(4) and (5)]. (b) Scaling of Landau time constants estimated from time series $r(t)$, such as those shown in (a), for onset ($\tau \propto \varepsilon^{-1.05}$, ●) and decay ($\tau \propto \varepsilon^{-0.92}$, ○) (theory: −1, solid line).

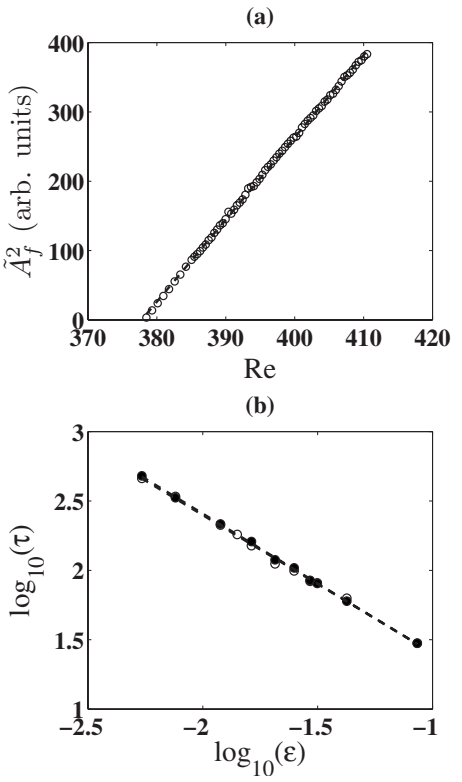

FIG. 5. (a) Scaling of measured final amplitude $\tilde{A}_f$ with Reynolds number and (b) of estimated time constants τ with ε of a wavy vortex flow with 16 Taylor cells at $\Gamma/N=1.3$. The linear fit (dashed line) verifies (a) the square-root law of amplitude $A \propto \sqrt{\varepsilon}$ and (b) for onset (●) and decay (○) the $\tau \propto 1/\varepsilon$ law of critical slowing down at a Hopf bifurcation.

is shown in Fig. 5(a). Excellent agreement with the theoretically proposed square-root law ($A_f \propto \sqrt{\varepsilon}$) is found in the experiments. The critical Reynolds number Re_c could be determined from a linear fit to $\mathrm{Re}_c=378.07$.

The scaling laws of the estimated time constant τ are represented in Fig. 5(b) for one particular onset ($\mathrm{Re}_i=344.8$) and decay ($\mathrm{Re}_i=410.6$). A linear fit reveals a scaling of $\tau \propto \varepsilon^{-1.007}$ for the onset and $\tau \propto \varepsilon^{-0.995}$ for the decay. Both scaling laws are in agreement with the theoretically predicted critical slowing down $\tau_l \propto 1/\varepsilon$.

It can be seen from Fig. 5(b) that the estimated time constants τ for onset and decay from these particular values of the initial amplitude are equal within the errors for any value of ε. A typical distribution of estimated time constants τ for onset and decay towards a fixed Re_f is shown in Fig. 6. The final Reynolds numbers $\mathrm{Re}_f=389.8$ are the same for all measurements, but the initial Reynolds numbers Re_i differ. It is apparent that within the measurement errors the estimated time constant τ of the wavy mode does not depend on the initial Reynolds number Re_i for a fixed Re_f. This is in agreement with predictions from Landau theory.

Our results are in agreement with the measurements of Pfister and Gerdts [24], but demonstrate further the independence of the time constants τ from the initial amplitude A_i. Therefore our extended experimental study confirms that a Hopf bifurcation can be considered as the appropriate theoretical model for the transition to wavy vortex flow.

B. Subharmonic small-jet mode

1. Oscillation amplitude

The small-jet mode differs in wave speed, axial periodicity, and depending on η also in the azimuthal wave number from the wavy mode, but the onset of both types to rotating waves has been modeled theoretically by a simple Hopf bifurcation. While this has been confirmed experimentally (partly among others) in Sec. V A for the wavy mode, our investigation of the onset of the small-jet mode reveals significant departures from the simple model.

In Fig. 7 a typical time series of the $\tilde{A}$ of the onset and decay towards a supercritical $\tilde{A}_f$ is shown. In contrast to the purly relaxating Landau dynamics of $\tilde{A}$ at the onset and decay of wavy vortices as depicted in Fig. 1, an overshooting for both the onset and the decay at the onset of a small-jet mode can be observed. For principle reasons such an amplitude dynamics cannot be governed by a one-dimensional Landau equation (1). The response of the amplitude has an oscillatory character, and this indicates that the amplitude of the small-jet mode is coupled to a further slow mode at least for this particular Re_f.

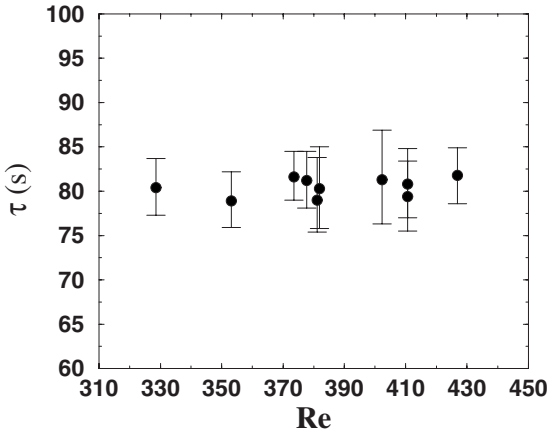

FIG. 6. Distribution of time constants τ estimated from transient dynamics towards wavy vortex flow at $\mathrm{Re}_f=389.8$ from different initial Reynolds numbers Re_i in a flow with 16 Taylor cells at $\Gamma/N=1.3$.

The overshooting which is clearly visible in the experimental time series of the transients can be observed if the final amplitude $\tilde{A}_f$ is sufficiently "large;" i.e., the final Reynolds number has a sufficiently large distance from the critical Reynolds number. However, even for smaller Reynolds numbers where the relaxation process appears again to be relaxating, a difference between the onset and decay of the small-jet mode can be found which is absent for wavy vortices. In Fig. 8 the distribution of estimated time constants τ for $\mathrm{Re}_f=427.6$ is shown. The departure from Landau theory can be clearly seen. The time constants estimated for the decay are significantly smaller than the ones for the onset, although they are equal within the fitting errors for each single process. This would not be the case if Landau theory would provide a sufficient description as it is the case for for the wavy mode (see Fig. 6).

Estimating Landau time constants τ by fitting Eq. (2) to experimental time series which are obviously not completely governed by Landau theory can be justified by two reasons:

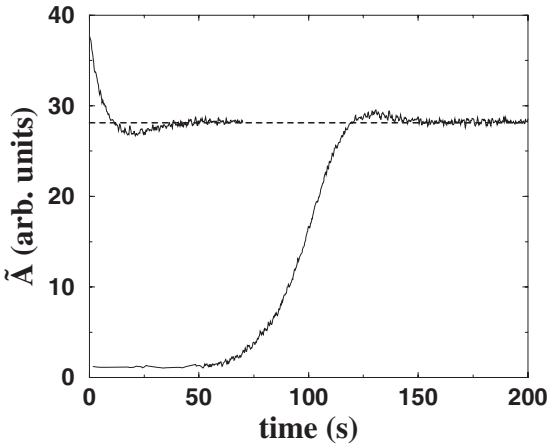

FIG. 7. (a) Transient dynamics of measured amplitude $\tilde{A}$ at the onset ($\mathrm{Re}_i=406.9$) and decay ($\mathrm{Re}_i=468.6$) of the subharmonic small-jet mode towards the supercritical final amplitude $\tilde{A}_f$ (dashed line) at $\mathrm{Re}_f=443.9$ in a flow with ten Taylor cells at $\Gamma/N=0.9$

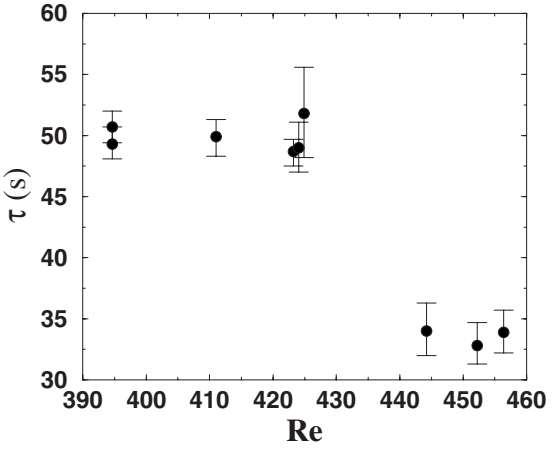

FIG. 8. Distribution of time constants τ estimated from transient dynamics towards the subharmonic small-jet mode at $\mathrm{Re}_f=427.6$ from different initial Reynolds numbers Re_i in a flow with ten Taylor cells at $\Gamma/N=0.9$.

First, the departure from Landau theory appears to be small in the time series (although it is significant) and becomes even smaller for decreasing A_f at least in the visual appearance from the measured response time series. Thus the success of a reasonable fit to more complicated models with more parameters seems questionable in particular also due to noise. Second, for the relevance of the departure for the bifurcation event it would be essential that this departure occur directly at the critical point and not only in a finite distance from it. The difference between onset and decay as shown in Fig. 8 for a finite distance from Re_c provides a qualitative measure for the departure from Landau theory. This measure gives also accurate information about the validity of Landau theory even very close to the critical Reynolds number as demonstrated in the case of the wavy mode.

The experimental scaling behavior at the onset of a small-jet mode in a ten-cell flow at $\Gamma/N=0.9$ is depicted in Fig. 9. Excellent agreement with the theoretically proposed square-root law of the final amplitude $A_f \propto \sqrt{\varepsilon}$ can be seen in Fig. 9(a). The critical Reynolds number could be determined to $\mathrm{Re}_c=420.27$ from a linear fit.

Critical slowing down could also be found at the onset of a small-jet mode with scaling laws for onset ($\tau=\tau_{onset}\varepsilon^{-0.993}$) and decay ($\tau=\tau_{decay}\varepsilon^{-0.992}$) being very close to the predicted $\tau \propto 1/\varepsilon$ from Landau theory. But the difference between the scaling factor τ_{onset} and τ_{decay} for onset and decay, respectively, remains within experimental accuracy even directly at the critical Reynolds number. The results are shown in Fig. 9(b). The initial Reynolds number was chosen to $\mathrm{Re}_i=394.6$ for the onset and $\mathrm{Re}_i=448.4$ for the decay. Note that only a single initial Reynolds number is sufficient for each process as can be seen from Fig. 8.

Similar experiments have been performed at the onset of a small-jet mode in flows having 6 and 16 cells at $\Gamma/N=0.9$. In each case a critical slowing down has been found, in agreement with Landau theory for both the onset with $\tau_6 \propto \varepsilon_6^{-1.036}$ and $\tau_{16} \propto \varepsilon_{16}^{-1.036}$ and for the decay with ($\tau_6 \propto \varepsilon_6^{-0.923}$ and $\tau_{16} \propto \varepsilon_{16}^{-0.989}$). However, the scaling factor for onset and decay differ in the same qualitative way as found in the ten-cell

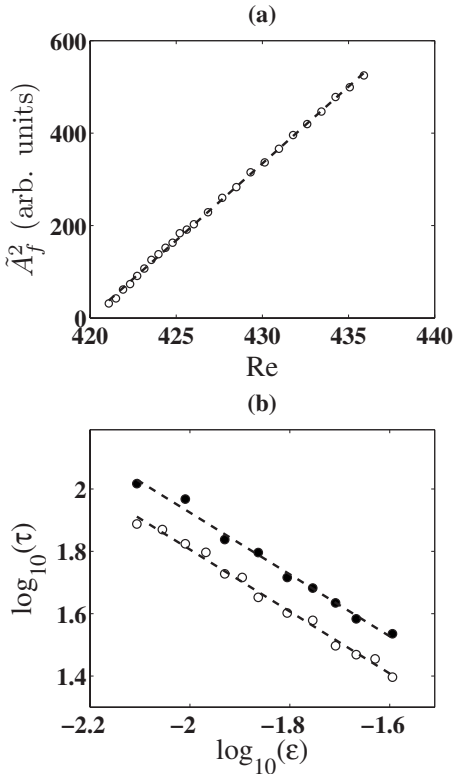

FIG. 9. (a) Scaling of the measured final amplitude $\tilde{A}_f$ with Reynolds number Re and (b) of estimated time constants τ with ε of a subharmonic small-jet mode in a flow with ten Taylor cells at $\Gamma/N=0.9$. The linear fit (dashed line) verifies (a) the square-root law of the amplitude $A \propto \sqrt{\varepsilon}$ and (b) for onset (●) and decay (○) the $\tau \propto 1/\varepsilon$ law of critical slowing down at a Hopf bifurcation. Note the offset between onset and decay in (b).

flow. In particular, the difference also remains for each Γ even at the critical Reynolds number. This difference indicates the influence of a further slow mode at the onset of a small-jet mode.

2. Imperfect reflection symmetry

The measured amplitude $\tilde{A}$ at the onset of a small-jet mode depicted in Fig. 7 is calculated from the mean of the (interpolated) time series $\tilde{A}_{max/min}(t)$ of oscillation maxima and minima. The corresponding time series of the difference $\chi=\tilde{A}_{max}(t)-\tilde{A}_{min}(t)$ between these two time series is shown in Fig. 10. A deterministic part in the dynamics of χ can be seen which shows a qualitatively similar behavior to the transient oscillatory response of the amplitude of the onset in Fig. 7. For the wavy mode such a difference could not be found in our experiments.

Due to the linear velocity profile of steady Taylor vortex flow in the axial middle of the system [21], the difference χ corresponds to a (small) shift of the oscillating outflow boundary towards the (in this case) lower-end boundary. This indicates that the upper half of the cells grows in size, while the lower half shrinks. Thus the flow becomes dynamically asymmetric with respect to the reflection symmetry as oscillations of the small-jet mode appear in the flow. The asymmetry remains for this supercritical Reynolds number even when the oscillation amplitude reaches its final value.

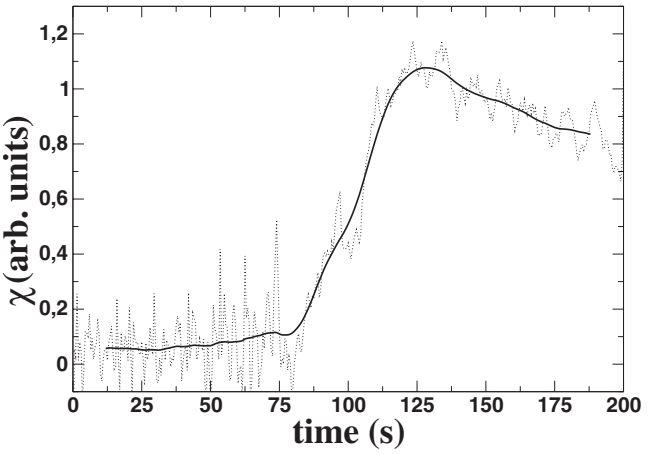

FIG. 10. (a) Transient dynamics of a measure χ for the asymmetry at the onset of a small-jet mode corresponding to the time series depicted in Fig. 7. A spline fit (solid line) is drawn to guide the eye.

The asymmetry at a (supercritical) final Reynolds number can be measured quantitatively from a distribution of the size λ of cells pairs. In Fig. 11(a) such a distribution is depicted for a 12-cell flow at $\Gamma/N=0.93$. In order to stress the influence of the small-jet mode, only the departure $\Delta\lambda$ from the cell pair sizes of steady Taylor vortices directly before onset is shown.

The sizes of cell pairs are determined from the axial position of the inflow boundaries. A mean of the radial position of the streamline with a zero-axial-velocity component provides an accurate measure for an inflow boundary. It is measured at seven different radial positions ($r=1,2,3,9,10,11,12$ mm) from the inner cylinder by a comparison of measured frequencies and frequency shift of the LDV.

The sizes of cell pairs of Taylor vortex flow at Re=537.2—i.e., directly before onset—are $\lambda_1=24.79$ mm, $\lambda_2=22.42$ mm, $\lambda_3=22.42$ mm, $\lambda_4=22.43$ mm, $\lambda_5=22.46$ mm, and $\lambda_6=24.83$ mm (cell pairs are numbered from bottom to top). Generally the sizes of steady Taylor vortices do not depend strongly on Reynolds number in this regime. For example, at a Reynolds number of 454.5 the sizes of each cell just differ by a maximum of 0.02 mm from the values given above. An asymmetry can already be found in steady Taylor vortices at Re=537.2, but with $\Delta\lambda=0.09$ mm it is very small. It can be seen from Fig. 11(a) that above the onset of a small-jet mode the sizes of the two end pairs (λ_1 and λ_6) decrease, while those of the bulk pairs ($\lambda_{2,3,4,5}$) increase with Reynolds number. Qualitatively the same behavior has been observed for the wavy mode [28].

The corresponding cell pairs in the bulk with respect to the reflection symmetry—i.e., $\Delta\lambda_2$ and $\Delta\lambda_5$ as well as $\Delta\lambda_3$ and $\Delta\lambda_4$—increase in size each by the same amount within the measurement accuracy. The end pairs, on the other hand, do not decrease by the same amount, but the pair at the bottom ($\Delta\lambda_1$) shrinks more than that at the top ($\Delta\lambda_6$). Thus the flow increases the asymmetry which can be measured by

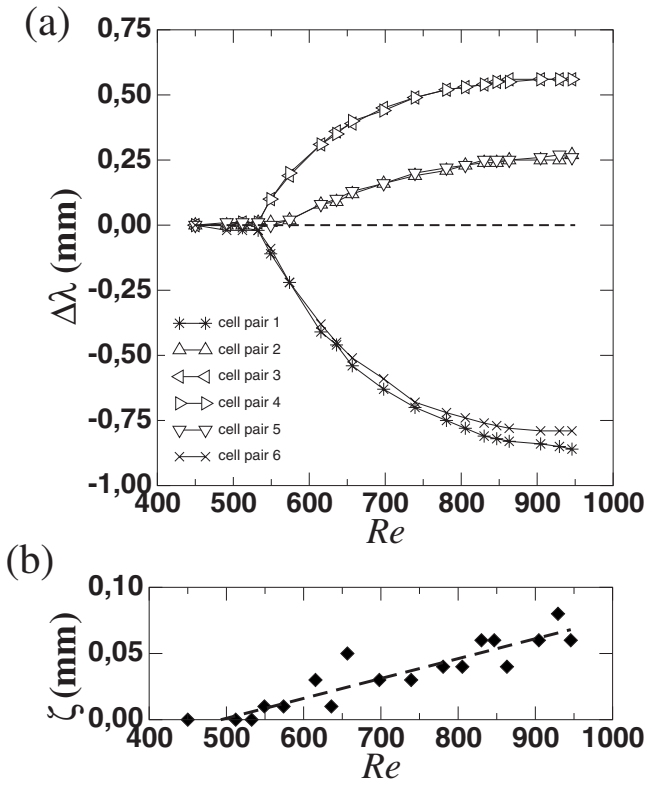

FIG. 11. (a) Departure $\Delta\lambda$ from the size of steady Taylor cell pairs due to the onset of a subharmonic small-jet mode in a flow with 12 Taylor cells at $\Gamma/N=0.93$. Sizes of end cell pairs reduce, while sizes of bulk cell pairs increase to higher Re. (b) Asymmetry ζ increased from the critical point almost linearly with Re as indicated by the linear fit (dashed line). This corresponds to an increasing difference in end pair sizes.

the difference in size between the upper and lower cell pairs; i.e., $\zeta=\Sigma_{i=0}^{2}(\Delta\lambda_{1+i}-\Delta\lambda_{6-i})$. The dependence of the asymmetry ζ of the Reynolds number is shown in Fig. 11(b). Although the absolute values of ζ are quite small a systematic increase of the asymmetry with Reynolds number can be found at the onset of the small-jet mode. The linear fit (dashed line) in Fig. 11(b) indicates a linear growth of asymmetry ζ with Re and thus a scaling law $\zeta \propto \varepsilon$.

VI. CONCLUSION

In this work we report on an experimental investigation on the onset of rotating waves in steady Taylor vortex flow. From our experimental results it can be concluded that imperfections which break the axial reflection symmetry of the flow can substantially alter the Hopf bifurcation towards wavy Taylor vortices.

Measurements of the nonlinear transient response and of the scaling behavior at the onset of two different kinds of rotating waves—i.e., the classical wavy mode and the axially subharmonic small-jet mode—are performed. While the wavy mode is found to be in excellent agreement with predictions from Landau theory, we reveal significant departures for the onset of the small-jet mode. We observe an oscillatory transient response of the slow amplitude at the Hopf bifurcation instead of relaxating Landau dynamics and an asymmetric response with respect to reflections about the axial midplane that is systematically connected to the oscillation amplitude.

Qualitatively similar behavior can be found in numerical simulations of a cusp-Hopf bifurcation model recently proposed by Harlim and Langford [11]. There, a nonlinear mode coupling between the oscillation amplitude and a slow but damped symmetry-breaking mode alters qualitatively the Hopf bifurcation. Such a coupling is a consequence of the imperfect reflection symmetry and would be absent in a system with perfect reflection symmetry .

In contrast to a pitchfork bifurcation, where the critical slowing down disappears, the critical dynamics of the Hopf bifurcation is only modified by imperfections. The similarity of numerical results with experimental observations suggests a similar mechanism acting in both systems; i.e., a coupling might occur due to (unavoidable experimental) imperfections of the axial reflection symmetry which modifies the critical dynamics and the scaling behavior of the Hopf bifurcation in Taylor-Couette flow.

Imperfections represent an important part of a realistic description of a bifurcation event in a physical system. They can cause new kinds of dynamical properties that do not occur in a symmetric model of the system as is found here for the classical onset of wavy Taylor vortices.

ACKNOWLEDGMENTS

We thank M. Wrage for assisting us with the measurements and H. Horak and W. Schumann for technical support.

[1] J. Guckenheimer and P. Holmes, *Nonlinear Oscillations, Dynamical Systems, and Bifurcations of Vector Fields* (Springer, New York, 1983).

[2] M. C. Cross and P. C. Hohenberg, Rev. Mod. Phys. **65**, 851 (1993); *Evolution of Spontaneous Structures in Dissipative Continous Systems*, edited by F. H. Busse and S. C. Müller (Springer, Berlin, 1998).

[3] M. Golubitsky, I. Stewart, and D. G. Schaeffer, *Singularities and Groups in Bifurcation Theory* (Springer, New York, 1988), Vol. 2.

[4] M. Golubitsky and D. G. Schaeffer, *Singularities and Groups in Bifurcation Theory* (Springer, New York, 1985), Vol. 1.

[5] J. Abshagen, G. Pfister, and T. Mullin, Phys. Rev. Lett. **87**, 224501 (2001).

[6] F. Marques, J. M. Lopez, and V. Iranzo, Phys. Fluids **14**, L33 (2002).

[7] *Hydrodynamic Instabilities and the Transition to Turbulence*, edited by H. L. Swinney and J. P. Gollub, *Topics in Applied Physics*, Vol. 45 (Springer, New York, 1981).

[8] E. L. Koschmieder, *Bénard Cells and Taylor Vortices* (Cambridge University Press, Cambridge, England, 1993); R. Tagg, Nonlinear Sci. Today **4**, 1 (1994); P. Chossat and G. Iooss, *The Taylor-Couette Problem* (Springer, Berlin, 1994); *The Nature of Chaos*, edited by T. Mullin (Oxford University Press, Oxford, 1994); *Physics of Rotating Fluids*, edited by C. Egbers and G. Pfister (Springer, Berlin, 2000).

[9] G. Dangelmayr and E. Knobloch, Nonlinearity **4**, 399 (1991); A. S. Landsberg and E. Knobloch, Phys. Rev. E **53**, 3579 (1996).

[10] J. D. Crawford and E. Knobloch, Nonlinearity **1**, 617 (1988); J. Abshagen, M. Heise, J. Langenberg, and G. Pfister, Phys. Rev. E **75**, 016309 (2007).

[11] J. Harlim and W. F. Langford, Int. J. Bifurcation Chaos Appl. Sci. Eng. **17**, 2547 (2007).

[12] M. Ipsen and P. G. Sørensen, Phys. Rev. Lett. **84**, 2389 (2000).

[13] A. Roxin and H. Riecke, Physica D **156**, 19 (2001).

[14] P. C. Matthews and S. M. Cox, Nonlinearity **13**, 1293 (2000); Physica D **175**, 196 (2003).

[15] P. Coullet and G. Iooss, Phys. Rev. Lett. **64**, 866 (1990).

[16] T. B. Benjamin, Proc. R. Soc. London, Ser. A **359**, 1 (1978); **359**, 27 (1978); T. Mullin, J. Fluid Mech. **121**, 207 (1982); K. A. Cliffe, J. J. Kobine, and T. Mullin, Proc. R. Soc. London, Ser. A **439**, 341 (1992).

[17] D. Coles, J. Fluid Mech. **21**, 385 (1965); T. Mullin and T. B. Benjamin, Nature (London) **288**, 567 (1980); A. Lorenzen, G. Pfister, and T. Mullin, Phys. Fluids **26**, 10 (1983); P. S. Marcus, J. Fluid Mech. **146**, 45 (1984); **146**, 69 (1984); T. Mullin, Phys. Rev. A **31**, 1216 (1985); C. D. Andereck, S. S. Lui, and H. L. Swinney, J. Fluid Mech. **164**, 155 (1986); M. Nagata, *ibid.* **188**, 585 (1988); W. S. Edwards, S. R. Beane, and S. Varme, Phys. Fluids A **3**, 1510 (1991); J. Antonijoan and J. Sánchez, Phys. Fluids **12**, 3147 (2000).

[18] U. Gerdts, J. von Stamm, T. Buzug, and G. Pfister, Phys. Rev. E **49**, 4019 (1994).

[19] G. Iooss, J. Fluid Mech. **173**, 273 (1986).

[20] C. A. Jones, J. Fluid Mech. **102**, 249 (1981); **157**, 135 (1985).

[21] J. von Stamm, U. Gerdts, T. Buzug, and G. Pfister, Phys. Rev. E **54**, 4938 (1996).

[22] R. J. Donnelly and K. W. Schwarz, Phys. Lett. **5**, 322 (1963); Proc. R. Soc. London, Ser. A **283**, 531 (1965); J. P. Gollub and M. H. Freilich, Phys. Rev. Lett. **33**, 1465 (1974); Phys. Fluids **19**, 618 (1976); G. P. Neitzel, J. Fluid Mech. **141**, 51 (1984); D. Hirshfeld and D. C. Rapaport, Phys. Rev. Lett. **80**, 5337 (1998); Phys. Rev. E **61**, R21 (2000).

[23] J. Abshagen, O. Meincke, G. Pfister, K. A. Cliffe, and T. Mullin, J. Fluid Mech. **476**, 335 (2003).

[24] G. Pfister and U. Gerdts, Phys. Lett. **83A**, 23 (1981).

[25] B. Hof and T. Mullin, Magnetohydrodynamics **37**, 119 (2001).

[26] G. Pfister, H. Schmidt, K. A. Cliffe, and T. Mullin, J. Fluid Mech. **191**, 1 (1988).

[27] W. F. Langford, in *Nonlinear Dynamics and Turbulence*, edited by G. I. Barenblatt, G. Iooss, and D. D. Joseph (Pitman, Boston, MA, 1983), p. 215.

[28] G. S. Bust, B. C. Dornblaser, and E. L. Koschmieder, Phys. Fluids **25**, 1243 (1985).